Modeling the role of alkanes, polycyclic aromatic hydrocarbons, and their oligomers in secondary organic aerosol formation

Havala O. T. Pye* and George A. Pouliot

US Environmental Protection Agency, National Exposure Research Laboratory, Research Triangle Park, North Carolina, USA

E-mail: pye.havala@epa.gov

Abstract

A computationally efficient method to treat secondary organic aerosol (SOA) from various length and structure alkanes as well as SOA from polycyclic aromatic hydrocarbons (PAHs) is implemented in the Community Multiscale Air Quality (CMAQ) model to predict aerosol concentrations over the United States. Oxidation of alkanes is predicted to produce more aerosol than oxidation of PAHs driven by relatively higher alkane emissions. SOA from alkanes and PAHs, although small in magnitude, can be a substantial fraction of the SOA from anthropogenic hydrocarbons, particularly in winter, and could contribute more if emission inventories lack intermediate volatility alkanes ($>C_{13}$) or if the vehicle fleet shifts toward diesel-powered vehicles. The SOA produced from oxidation of alkanes correlates well with ozone and odd oxygen in many locations, but the lower correlation of anthropogenic oligomers with odd oxygen indicates that models may need additional photochemically dependent pathways to low-volatility SOA.

*To whom correspondence should be addressed

1

Introduction

Organic aerosol is a highly uncertain and important component of particulate matter with implications for public health, visibility, and climate. Until recently, atmospherically relevant yields of secondary organic aerosol (SOA) from alkanes (1) and PAHs (2) had not been measured. Long-chain (C_6 to C_{19}) alkanes and small (2-4 ring) polycyclic aromatic hydrocarbons (PAHs), many of which are intermediate volatility organic compounds (IVOCs) (3), can produce secondary organic aerosol (SOA) in relatively high amounts (2, 4–6). The yield of SOA from an alkane can range from a few percent or less for small compounds such as cyclohexane and n-octane up to more than 90% for large compounds like cyclopentadecane (7). Small PAHs, such as naphthalene and methyl naphthalenes, have been found to produce SOA with yields up to 73% (2). Molecular markers of naphthalene oxidation are found in ambient aerosol (8), and observations from a variety of locations imply that alkanes may be an important source of SOA (9–11).

Bottom-up modeling studies indicate the contribution of anthropogenic hydrocarbons to ambient organic aerosol is on the order of a few tenths of a $\mu g/m^3$ at the surface and about 3 Tg/yr or 10% of the global SOA production rate (12–14). Top-down estimates indicate that missing sources of SOA may more closely resemble the existing anthropogenic SOA in models and the SOA production rate should be on the order of 100 Tg/yr or more (15). The contributions of anthropogenic and biogenic hydrocarbons as well as their interactions in terms of SOA production should be carefully considered.

Most traditional air quality model frameworks, which tend to underestimate ambient organic aerosol loadings (16–18), either do not treat alkanes and PAHs as aerosol precursors or represent them with low yields. Emissions of IVOC alkanes and PAHs, although perhaps small in magnitude in current emission inventories, could be the largest contributors to SOA from anthropogenic VOCs. In this work, a parameterization for SOA from alkanes that captures the dependence of yield on parent hydrocarbon structure is developed. Combined with a parameterization for SOA from PAHs, the contribution of alkanes and PAHs to organic aerosol over the U.S. is predicted and evaluated in terms of its correlation with ozone and odd oxygen.

2

Model Implementation

Chemical Transport Model

The Community Multiscale Air Quality (CMAQ) model version 5.0 simulates organic aerosol from primary sources (19), monoterpenes, sesquiterpenes, isoprene, and aromatics as well as aerosol produced by aqueous processes (13) and is updated in this work to include additional aerosol from alkanes and PAHs (see the supporting information for a description of pathways that were removed from CMAQ 5.0 to prevent double counting in this work). The model is employed with SAPRC07TB chemistry (20, 21) and the AERO6 aerosol module to simulate the continental United States at 12km by 12km horizontal resolution using 35 vertical layers and meteorology from the Weather Research and Forecasting (WRF) model. Emissions are based on year 2006 (using the 2005 EPA National Emission Inventory (NEI), available at www.epa.gov/ttnchief1/net/2005inventory.html, and BEIS v3.14). Following ten days of spinup, concentrations are simulated for one month in winter (January 11 to February 10, 2006) and one month in summer (July 2006).

SOA Yields

Chain length affects the yield of alkane aerosol through its influence on the volatility of products formed (4, 22). SOA from very large alkanes likely comes from first generation oxidation products while smaller alkanes produce SOA through first and higher generation chemistry including reactions of dihydrofurans (4, 22). The structure of the alkane (linear, branched, or cyclic) also impacts yields as a result of competition between isomerization and decomposition of the alkoxy radical (7, 23). The isomerization pathway can lead to further functionalization and products with low volatility. For alkanes in which the alkoxy radical is branch adjacent, decomposition competes with isomerization and results in lower SOA yields. For compounds with high ring strain (cyclooctane, cyclodecane), decomposition becomes more favorable, but tends to produce ring-opening products with an additional carbonyl group and higher SOA yields compared to linear alkanes (7, 24). Thus the parent alkane hydrocarbon identity affects both the composition and

3

yield of SOA.

Although the yield of SOA from alkanes is a function of parent hydrocarbon identity, individual alkanes will likely not be explicitly represented in models due to a lack of information on emissions and the computational burden of tracking additional species. Here, a parameterization for n-dodecane ($C_{12}H_{26}$) SOA and a method to treat alkanes of varying length and structure is developed. Linear dodecane is chosen as a surrogate compound for alkane SOA because it has been examined in a number of laboratory studies (1, 4), falls in the middle of the range of alkane compounds considered in terms of size and volatility, and is a significant portion of alkane emissions from sources such as diesel exhaust (25). High-NO$_x$ n-dodecane oxidation data from Presto et al. (1) and Lewandowski et al., *in preparation* (Lewandowski et al., SOA formation yields from the linear C_8 through C_{14} alkanes, *in preparation*) are fit with an Odum 2-product curve (Table 1) and this yield curve is applied over all NO$_x$ regimes. The Lewandowski et al. concentrations range from about 10 to 200 μg/m^3, and the organic aerosol loadings over which the two data sets overlap (10-20 μg/m^3) suggest that yields can vary between experiments by approximately 50% (most likely due to different NO$_x$ levels). Changes in UV intensity can also be a source of variation in chamber yields (1).

Naphthalene accounts for a significant fraction of PAHs emitted in the gas phase and is used as a surrogate species for all SOA from gas-phase PAHs. Oxidation under high-NO$_x$ or low-NO$_x$ conditions leads to ring-opening or ring-retaining compounds respectively (8). As a result, yields under low-NO$_x$ conditions tend to be relatively constant with respect to loading, indicative of nonvolatile SOA, while high-NO$_x$ SOA is semivolatile (2, 26). The yield of SOA is parameterized based on the fate of the peroxy radical (RO$_2$ reaction with HO$_2$ vs NO) and the Odum 2-product fit from Chan et al. (2) and shown in Table 1.

In the model, semivolatile SOA from alkanes and PAHs undergoes particle-phase reaction with a half-life of 20 hours converting it to nonvolatile SOA following previous work (13, 27). Work by Lim and Ziemann (24) indicates that oligomers likely do form in alkane SOA systems, particularly for oxidation of cyclic alkanes. High molecular weight products like oligomers are not observed

in naphthalene oxidation experiments in the presence of ammonium sulfate but an organic sulfonic acid is produced in the particle (8). Only the high-NO_x PAH SOA undergoes the particle-phase reaction in the model since the low-NO_x pathway produces nonvolatile aerosol, thus oligomerization of the PAH SOA in the model is expected to be relatively minor. See Figure S1 for a schematic of the SOA treatment.

Emissions

C_6 and larger cyclic and C_8 and larger linear or branched alkanes are considered SOA precursors (7). Alkanes with 20 carbons or more may be emitted in the gas and particle phase, and are not explicitly treated in this work. The alkane emissions are weighted relative to *n*-dodecane to account for the fact that individual alkanes have different yields. For example, if the yield of SOA from *n*-tetradecane is observed to be 2.9 times as high as the yield from *n*-dodecane at a similar organic aerosol loading, the emission rate is multiplied by 2.9 to create a dodecane-equivalent emission rate to be used with the empirically-based dodecane yield parameterization. Note that this approach is an approximation limited by the fact that alkane SOA yield data are generally available at only one or a limited set of loadings (some of which may not be atmospherically relevant) and tracking the identity of each parent alkane from emission through SOA formation is too computationally expensive in a chemical transport model. When information for a given alkane and dodecane are available in the same study over a range of organic aerosol concentrations, a loading of 5 $\mu g/m^3$ is used to calculate the relative yield. Yields are nonlinear with organic aerosol loading, but Presto et al. (*1*) experiments with *n*-pentadecane and *n*-heptadecane indicate that the relative yield does not deviate from the 5 $\mu g/m^3$ value by more than 20% for aerosol concentrations between 1.7 and 20 $\mu g/m^3$.

The SOA yield for various alkanes relative to *n*-dodecane is shown in Figure 1 and Table S1. For simplicity, branched compounds are assumed to form half as much SOA as linear compounds with the same number of carbons which corresponds to the effect expected for 1.5 methyl groups in a 12 carbon alkane (7). All cyclic compounds are treated as if they do not contain branches

although work by Lim and Ziemann found that yields of cyclic compounds with branches could be higher or lower than a linear alkane with the same number of carbons (7).

To determine the dodecane-equivalent emissions, domain-wide emissions are speciated using source-specific profiles from SPECIATE version 4.2 (28). The C_6 to C_{19} cyclic and C_8 to C_{19} linear and branched emissions (Figure 2) are then weighted according to the yield relative to dodecane. Figure 2 indicates a portion of the total VOC emissions that were not identified in SPECIATE (includes species like "aggregated VOCs" or "undefined VOC") and totals 466 Mg/yr.

Following a similar approach for small polycyclic aromatic hydrocarbons, the NEI and SPE-CIATE are used to identify the emissions that behave as a PAH. No adjustment is made for different size or structure PAHs although larger PAHs may have higher SOA yields than the surrogate species naphthalene.

Results and Discussion

Emissions

The alkane SOA precursor emissions (C_6 and larger cyclic and C_8 and larger linear and branched compounds) are about 1500 Mg/yr as depicted in Figure 2. The emission rate falls off quickly with increasing carbon number starting at C_{13} which is similar to the fuel composition and emission profile for gasoline powered vehicles (29) but in contrast to the diesel profile which tends to have relatively similar emissions for C_{12} through C_{19} linear compounds (25). Conversion to a dodecane-equivalent emission rate results in a 53% decrease in the alkane SOA precursor emission rate and reflects the fact that compounds with yields lower than dodecane tend to dominate the emission inventory.

The decrease in emission rate with increasing carbon number may reflect the true emission profile or limitations in the collection and detection of certain compounds. For diesel exhaust (25), unknown compounds contribute 20.5% of the total VOC mass and include aliphatic branched and cyclic hydrocarbons. Remapping the unknown emissions shown in Figure 2 to SOA alkane

6

precursor species would increase the total SOA precursor emission rate from diesel vehicles by 30%. If the unknowns were more likely to be C_{13} or longer alkanes, the dodecane-equivalent emission rate would also be much higher and could have a significant influence on ambient SOA levels. The "unknown" emission rate is likely a lower estimate on the amount of unspeciated emissions since many profiles in SPECIATE are normalized to the total speciated emissions. For example, in the case of residential wood combustion (30), 6.5% of the VOC mass that makes up the unresolved complex mixture is not included in SPECIATE. The NEI, which supplies the total VOC emission rate, is another source of uncertainty.

Domain-wide, the gas-phase PAH emissions are estimated to be less than 100 Mg/yr, which is significantly smaller than the alkane SOA precursor rate. Naphthalene emissions come mostly from non-point sources such as residential wood combustion with smaller contributions from mobile and point sources.

Aerosol Contribution

Figure 3 shows the estimated contribution to alkane SOA by carbon number. Note that cyclic compounds are assumed to be more efficient aerosol producers than linear or branched alkanes with the same number of carbons. The longest chain alkanes considered, particularly C_{13} through C_{17} compounds are effective SOA precursors, especially when placed in the context of their emission rate. Compared to the emissions (Figure 2), branched compounds such as branched C_8 compounds are diminished in their importance and long-chain alkanes become more important. With the current emission inventory and information available from SPECIATE, C_{13} and longer alkanes are predicted to contribute about 13% of the alkane SOA despite making up less than 2% of the alkane SOA precursor emissions. With additional IVOC emissions, the contribution could be higher (31).

Figure 4 shows the predicted contribution to surface level organic aerosol from oxidation of alkanes and PAHs. The first two columns represent SOA directly formed from alkanes and PAHs respectively. (In general, when referring to the modeled species alkane SOA or PAH SOA, the oligomers are excluded. If the oligomers are included, they will be explicitly mentioned.) The

7

third column represents oligomers formed from alkanes and PAHs and was estimated by taking the difference in predicted anthropogenic oligomer concentration between a run with alkane and PAH SOA and one without. Alkanes are predicted to be a greater contributor to surface level organic aerosol concentrations than PAHs, and about half of the new aerosol may come from oligomerization. The final column (Figure 4) shows the percent contribution of SOA from alkanes, PAHs, and their oligomers to SOA from all anthropogenic hydrocarbons including light aromatics. Since GEOS-Chem, which provides the aerosol boundary conditions for this work, does not treat SOA from alkanes and PAHs, alkane and PAH SOA is set to zero at the boundary resulting in a low contribution of those species to SOA near the edge of the domain. On a fractional basis, the alkanes and PAHs are actually a greater contributor to winter-time organic aerosol concentrations than summer concentrations since light aromatic SOA yields may be higher in summer as the RO_2+HO_2 pathway producing nonvolatile aerosol becomes more favorable (12). In addition, since alkane SOA is semivolatile, aerosol formation will be more favorable at lower temperatures. In summer and winter, SOA from alkanes and PAHs can make up 20-30% of anthropogenic SOA on average.

Even with the new aerosol from alkanes and PAHs, the model continues to underestimate OC at high concentrations and during the summer except at very low loadings compared to observations from the Chemical Speciation Network (CSN) which contains a number of urban monitoring sites. At low loadings in winter, the model can overestimate concentrations of OC (Figure S4).

Correlation With Odd Oxygen

Ozone and SOA are both photochemically produced species and observations indicate that organic aerosol, particularly ambient surrogates for SOA such as oxygenated organic aerosol (OOA), can be well correlated with odd oxygen, O_x, ($O_x=O_3+NO_2$) (32–34). Reaction of first generation alkane oxidation products such as dihydrofurans with ozone might also be responsible for significant SOA production (10). Here, the relationship between SOA from alkanes and ozone as well as odd oxygen is examined to determine the degree to which they are correlated in the model.

8

Figure 5 shows r^2 (square of Pearson correlation coefficient) for hourly averaged predictions of alkane SOA and odd oxygen during July 2006. The model indicates that alkane SOA can be highly correlated with odd oxygen in the model with some areas exceeding a r^2 of 0.7. Many of these correlations are likely meteorologically driven, such as those over Lake Michigan where a stable marine boundary layer often exists at night (35). Many cities (source regions) show relatively high correlations between alkane SOA and O_x, but there is relatively poor correlation between total SOA and O_x in the model (values usually less than $r^2 \approx 0.4$). Aerosol from light aromatics shows better correlation with O_x than total SOA but usually slightly less correlation than the alkane SOA, particularly in Atlanta, St. Louis, and parts of California. The correlation for light aromatic aerosol can be higher than that for alkane SOA in some outflow regions as aromatics move from high-NO_x to low-NO_x regimes and aromatic SOA products shift from semivolatile to nonvolatile species.

Since the model used here lacks an explicit dependence of alkane SOA on ozone concentrations (alkane oxidation by OH is assumed to be the rate limiting step for formation of the semivolatiles), the correlation in the model is not a result of a direct interaction of the alkane SOA precursors or intermediate products and ozone. At Scripps Pier in La Jolla, California, USA carboxylic acid functional groups, potentially from alkane oxidation, were observed to correlate well with ozone ($r^2 \approx 0.5$) (9). The modeled alkane SOA sampled at the same frequency and duration and normalized to CO (36), shows a similar correlation with ozone ($r^2 = 0.55$) as the observations. The correlation of modeled alkane SOA with ozone is higher than the correlation with OH ($r^2 = 0.36$) likely reflecting the longer lifetime of SOA compared to OH. The correlation with ozone in the model lends support to the hypothesis that alkane oxidation by OH produces SOA consistent with the carboxylic acid functional group surrogate, but does not exclude an intermediate role for ozone in alkane SOA production. However, if oxidation of dihydrofurans by ozone is the dominant pathway to alkane SOA (10), the SOA yield based on OH in the model used here, may need to be confirmed.

Monoterpenes and sesquiterpenes in the model produce aerosol directly from an ozone oxidation pathway. The alkane-O_x correlation presumably is sensitive to the presence of terpenes if

9

terpene ozonolysis creates a larger organic mass into which alkane SOA can partition. Examining the r^2 of monoterpene SOA compared to that of alkane SOA indicates that the monoterpene SOA is not the driving factor for the alkane SOA correlation with odd oxygen (particularly in urban areas and California).

Figure 6 shows the diurnal variation in SOA from alkanes, OH, and ozone in Bakersfield, California in the San Joaquin Valley. The daytime alkane SOA is correlated to a slightly greater degree with ozone (r^2=0.31) than OH (r^2=0.25), but, O_3 and OH are more greatly correlated with each other (r^2=0.47). (Normalized to CO (to minimize effects of meteorology and emission strength) the magnitude of the correlation of alkane SOA with O_3 and OH increases to about $r^2 \approx 0.39$ in each case.) A portion of the SOA from alkanes is converted to oligomers which lose their specific parent hydrocarbon identity in the model and are not included in Figure 6 or the above alkane SOA correlations. The modeled anthropogenic oligomer concentration (monthly median) varies by around $\pm 10\%$ during the daytime in Bakersfield, peaking in the middle of the day and has a low r^2 with daytime ozone (0.11). Wood et al. (34) found that the AMS semivolatile oxygenated organic aerosol (SV-OOA) factor did not correlate as well with odd oxygen as did the low-volatility oxygenated organic aerosol (LV-OOA) in Mexico City. For the same time period, Herndon et al. (37), however, noted that the magnitude of the slope of OOA vs O_x was steeper for "less aged" OOA. If alkane SOA and anthropogenic oligomers are considered the model equivalent of SV-OOA and LV-OOA, the Wood et al. (34) trend implies that the the model process for converting semivolatile to low-volatility organic aerosol (or formation of low-volatility organic aerosol in general) may need more of a diurnal or photochemical dependence than the current oligomerization pathway allows.

Future Directions

SOA from alkanes parameterized by reaction with OH leads to aerosol that is well correlated with odd oxygen, consistent with observations of SOA surrogates. The contribution of alkane and PAH oxidation to ground level organic aerosol is predicted to be 20 to 30 percent of SOA

from anthropogenic hydrocarbons which could dominate in urban locations with large populations. Semivolatile or intermediate volatility emissions not included in current inventories would be effective SOA precursors and increase the contribution of alkanes and PAHs to SOA. In addition, allowing for evaporation and subsequent oxidation of existing primary organic aerosol or oxidation of semivolatile SOA in the gas phase (*31*) may lead to even greater amounts of SOA from anthropogenic hydrocarbons. Improved speciation of VOC emissions would produce better estimations of alkane and PAH SOA.

The trend in correlation of SV-OOA and LV-OOA with odd oxygen can serve as a method to evaluate model processes. CMAQ accomplishes conversion to lower volatility species via an oligomerization-like particle-phase reaction that produces aerosol that is generally less correlated with odd oxygen than the semivolatile aerosol from which it was produced. If ambient organic aerosol eventually converges to LV-OOA (*38*), OOA and O_x are well correlated in the ambient, and the laboratory SOA on which models are based is most similar to SV-OOA (*39, 40*), additional pathways to produce LV-OOA from anthropogenic hydrocarbons in models are needed.

Acknowledgement

Supporting Information Available

Details on the implementation of emissions, pathways removed from CMAQ 5.0, values from Figure 1, a comparison to CSN observations, and surface level SOA predictions are available in the supplemental material. This material is available free of charge via the Internet at http:

//pubs.acs.org/.

References

(1) Presto, A. A.; Miracolo, M. A.; Donahue, N. M.; Robinson, A. L. Secondary organic aerosol formation from high-NO_x photo-oxidation of low volatility precursors: *n*-alkanes. *Environ. Sci. Technol.* **2010**, *44*, 2029–2034.

(2) Chan, A. W. H.; Kautzman, K. E.; Chhabra, P. S.; Surratt, J. D.; Chan, M. N.; Crounse, J. D.; Kurten, A.; Wennberg, P. O.; Flagan, R. C.; Seinfeld, J. H. Secondary organic aerosol formation from photooxidation of naphthalene and alkylnaphthalenes: Implications for oxidation of intermediate volatility organic compounds (IVOCs). *Atmos. Chem. Phys.* **2009**, *9*, 3049–3060.

(3) Donahue, N. M.; Robinson, A. L.; Stanier, C. O.; Pandis, S. N. Coupled partitioning, dilution, and chemical aging of semivolatile organics. *Environ. Sci. Technol.* **2006**, *40*, 2635–2643.

(4) Lim, Y. B.; Ziemann, P. J. Products and mechanism of secondary organic aerosol formation from reactions of n-alkanes with OH radicals in the presence of NO_x. *Environ. Sci. Technol.* **2005**, *39*, 9229–9236.

(5) Chacon-Madrid, H. J.; Donahue, N. M. Fragmentation vs. functionalization: Chemical aging and organic aerosol formation. *Atmos. Chem. Phys.* **2011**, *11*, 10553–10563.

(6) Ziemann, P. J. Effects of molecular structure on the chemistry of aerosol formation from the OH-radical-initiated oxidation of alkanes and alkenes. *Int. Rev. Phys. Chem.* **2011**, *30*, 161–195.

(7) Lim, Y. B.; Ziemann, P. J. Effects of molecular structure on aerosol yields from OH radical-initiated reactions of linear, branched, and cyclic alkanes in the presence of NO_x. *Environ. Sci. Technol.* **2009**, *43*, 2328–2334.

(8) Kautzman, K. E.; Surratt, J. D.; Chan, M. N.; Chan, A. W. H.; Hersey, S. P.; Chhabra, P. S.; Dalleska, N. F.; Wennberg, P. O.; Flagan, R. C.; Seinfeld, J. H. Chemical composition of gas- and aerosol-phase products from the photooxidation of naphthalene. *J. Phys. Chem. A* **2010**, *114*, 913–934.

(9) Liu, S.; Day, D. A.; Shields, J. E.; Russell, L. M. Ozone-driven photochemical formation of carboxylic acid groups from alkane groups. *Atmos. Chem. Phys.* **2011**, *11*, 8321–8341.

(10) Russell, L. M.; Bahadur, R.; Ziemann, P. J. Identifying organic aerosol sources by comparing functional group composition in chamber and atmospheric particles. *Proc. Nat. Acad. Sci. U.S.A.* **2011**, *108*, 3516–3521.

(11) de Gouw, J. A. et al. Organic aerosol formation downwind from the deepwater horizon oil spill. *Science* **2011**, *331*, 1295–1299.

(12) Henze, D. K.; Seinfeld, J. H.; Ng, N. L.; Kroll, J. H.; Fu, T. M.; Jacob, D. J.; Heald, C. L. Global modeling of secondary organic aerosol formation from aromatic hydrocarbons: High- vs. low-yield pathways. *Atmos. Chem. Phys.* **2008**, *8*, 2405–2420.

(13) Carlton, A. G.; Bhave, P. V.; Napelenok, S. L.; Edney, E. D.; Sarwar, G.; Pinder, R. W.; Pouliot, G. A.; Houyoux, M. Model representation of secondary organic aerosol in CMAQv4.7. *Environ. Sci. Technol.* **2010**, *44*, 8553–8560.

(14) Pye, H. O. T.; Chan, A. W. H.; Barkley, M. P.; Seinfeld, J. H. Global modeling of organic aerosol: The importance of reactive nitrogen (NO_x and NO_3). *Atmos. Chem. Phys.* **2010**, *10*, 11261–11276.

(15) Heald, C. L. et al. Exploring the vertical profile of atmospheric organic aerosol: Comparing 17 aircraft field campaigns with a global model. *Atmos. Chem. Phys.* **2011**, *11*, 12673–12696.

(16) Foley, K. M.; Roselle, S. J.; Appel, K. W.; Bhave, P. V.; Pleim, J. E.; Otte, T. L.; Mathur, R.; Sarwar, G.; Young, J. O.; Gilliam, R. C.; Nolte, C. G.; Kelly, J. T.; Gilliland, A. B.; Bash, J. O.

13

Incremental testing of the Community Multiscale Air Quality (CMAQ) modeling system version 4.7. *Geosci. Model Dev.* **2010**, *3*, 205–226.

(17) Volkamer, R.; Jimenez, J. L.; San Martini, F.; Dzepina, K.; Zhang, Q.; Salcedo, D.; Molina, L. T.; Worsnop, D. R.; Molina, M. J. Secondary organic aerosol formation from anthropogenic air pollution: Rapid and higher than expected. *Geophys. Res. Lett.* **2006**, *33*.

(18) de Gouw, J. A. et al. Sources of particulate matter in the northeastern United States in summer: 1. Direct emissions and secondary formation of organic matter in urban plumes. *J. Geophys. Res.-Atmos.* **2008**, *113*.

(19) Simon, H.; Bhave, P. V. Simulating the degree of oxidation in atmospheric organic particles. *Environ. Sci. Technol.* **2012**, *46*, 331–339.

(20) Hutzell, W. T.; Luecken, D. J.; Appel, K. W.; Carter, W. P. L. Interpreting predictions from the SAPRC07 mechanism based on regional and continental simulations. *Atmos. Environ.* **2012**, *46*, 417–429.

(21) Carter, W. P. L. Development of the SAPRC-07 chemical mechanism. *Atmos. Environ.* **2010**, *44*, 5324–5335.

(22) Jordan, C. E.; Ziemann, P. J.; Griffin, R. J.; Lim, Y. B.; Atkinson, R.; Arey, J. Modeling SOA formation from OH reactions with C_8-C_{17} *n*-alkanes. *Atmos. Environ.* **2008**, *42*, 8015–8026.

(23) Atkinson, R. Rate constants for the atmospheric reactions of alkoxy radicals: An updated estimation method. *Atmos. Environ.* **2007**, *41*, 8468–8485.

(24) Lim, Y. B.; Ziemann, P. J. Chemistry of secondary organic aerosol formation from OH radical-initiated reactions of linear, branched, and cyclic alkanes in the presence of NO_x. *Aerosol Sci. Technol.* **2009**, *43*, 604–619.

(25) Schauer, J. J.; Kleeman, M. J.; Cass, G. R.; Simoneit, B. R. T. Measurement of emissions

from air pollution sources: 2. C_1 through C_{30} organic compounds from medium duty diesel trucks. *Environ. Sci. Technol.* **1999**, *33*, 1578–1587.

(26) Shakya, K. M.; Griffin, R. J. Secondary organic aerosol from photooxidation of polycyclic aromatic hydrocarbons. *Environ. Sci. Technol.* **2010**, *44*, 8134–8139.

(27) Kalberer, M.; Paulsen, D.; Sax, M.; Steinbacher, M.; Dommen, J.; Prevot, A. S. H.; Fisseha, R.; Weingartner, E.; Frankevich, V.; Zenobi, R.; Baltensperger, U. Identification of polymers as major components of atmospheric organic aerosols. *Science* **2004**, *303*, 1659–1662.

(28) Simon, H.; Beck, L.; Bhave, P. V.; Divita Jr., F.; Hsu, Y.; Luecken, D.; Mobley, J. D.; Pouliot, G. A.; Reff, A.; Sarwar, G.; Strum, M. The development and uses of EPA's SPECIATE database. *Atmos. Poll. Res.* **2010**, *1*, 196–206.

(29) Schauer, J. J.; Kleeman, M. J.; Cass, G. R.; Simoneit, B. R. T. Measurement of emissions from air pollution sources: 5. C_1-C_{32} organic compounds from gasoline-powered motor vehicles. *Environ. Sci. Technol.* **2002**, *36*, 1169–1180.

(30) Schauer, J. J.; Kleeman, M. J.; Cass, G. R.; Simoneit, B. R. T. Measurement of emissions from air pollution sources: 3. C_1-C_{29} organic compounds from fireplace combustion of wood. *Environ. Sci. Technol.* **2001**, *35*, 1716–1728.

(31) Robinson, A. L.; Donahue, N. M.; Shrivastava, M. K.; Weitkamp, E. A.; Sage, A. M.; Grieshop, A. P.; Lane, T. E.; Pierce, J. R.; Pandis, S. N. Rethinking organic aerosols: Semivolatile emissions and photochemical aging. *Science* **2007**, *315*, 1259–1262.

(32) Lanz, V. A.; Alfarra, M. R.; Baltensperger, U.; Buchmann, B.; Hueglin, C.; Prevot, A. S. H. Source apportionment of submicron organic aerosols at an urban site by factor analytical modelling of aerosol mass spectra. *Atmos. Chem. Phys.* **2007**, *7*, 1503–1522.

(33) Matsui, H.; Koike, M.; Takegawa, N.; Kondo, Y.; Griffin, R. J.; Miyazaki, Y.; Yokouchi, Y.; Ohara, T. Secondary organic aerosol formation in urban air: Temporal variations and possible contributions from unidentified hydrocarbons. *J. Geophys. Res.-Atmos.* **2009**, *114*.

(34) Wood, E. C. et al. Investigation of the correlation between odd oxygen and secondary organic aerosol in Mexico City and Houston. *Atmos. Chem. Phys.* **2010**, *10*, 8947–8968.

(35) Spak, S. N.; Holloway, T. Seasonality of speciated aerosol transport over the Great Lakes region. *J. Geophys. Res.-Atmos.* **2009**, *114*.

(36) DeCarlo, P. F.; Ulbrich, I. M.; Crounse, J.; de Foy, B.; Dunlea, E. J.; Aiken, A. C.; Knapp, D.; Weinheimer, A. J.; Campos, T.; Wennberg, P. O.; Jimenez, J. L. Investigation of the sources and processing of organic aerosol over the Central Mexican Plateau from aircraft measurements during MILAGRO. *Atmos. Chem. Phys.* **2010**, *10*, 5257–5280.

(37) Herndon, S. C. et al. Correlation of secondary organic aerosol with odd oxygen in Mexico City. *Geophys. Res. Lett.* **2008**, *35*.

(38) Jimenez, J. L. et al. Evolution of organic aerosols in the atmosphere. *Science* **2009**, *326*, 1525–1529.

(39) Ng, N. L. et al. Organic aerosol components observed in Northern Hemispheric datasets from Aerosol Mass Spectrometry. *Atmos. Chem. Phys.* **2010**, *10*, 4625–4641.

(40) Presto, A. A.; Miracolo, M. A.; Kroll, J. H.; Worsnop, D. R.; Robinson, A. L.; Donahue, N. M. Intermediate-volatility organic compounds: A potential source of ambient oxidized organic aerosol. *Environ. Sci. Technol.* **2009**, *43*, 4744–4749.

Table 1: SOA parameterization for alkanes (*n*-dodecane) and PAHs (naphthalene) at 298 K. The OM/OC and enthalpy of vaporization values (ΔH) are based on Kleindienst et al., The formation of SOA and chemical tracer compounds from the photooxidation of naphthalene and its methyl analogs in the presence and absence of nitrogen oxides, *submitted* and Lewandowski et al., SOA formation yields from the linear C_8 through C_{14} alkanes, *in preparation*. The aerosol molecular weight is set to be consistent with the OM/OC. Naphthalene is assumed to form nonvolatile aerosol under low-NO_x conditions based on the work of Chan et al. (*2*).

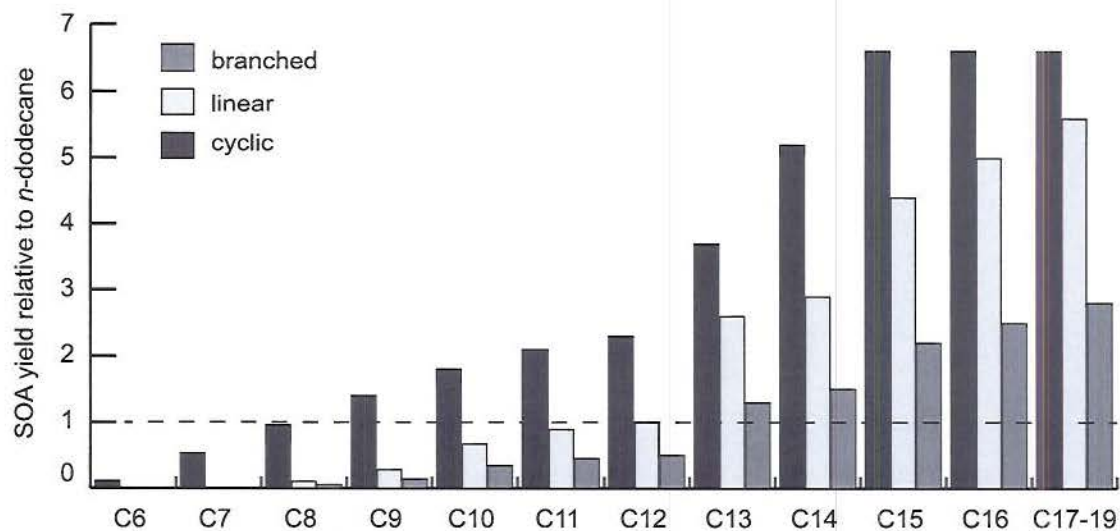| Parent hydrocarbon	α [$\mu g/\mu g$]	C^* [$\mu g/m^3$]	Mwt [g/mol]	OM/OC	ΔH [kJ/mol]	Reference
alkane	0.03	0.147	168	1.17	53	Lewandowski et al., *in preparation*
	0.22	51.9	168	1.17	53	
PAH (high-NO_x)	0.21	1.66	243	2.03	18	2, Kleindienst et al., *submitted*
	1.07	264.7	243	2.03	18	
PAH (low-NO_x)	0.73	NA	243	2.03	NA	2, Kleindienst et al., *submitted*

Figure 1: Ratio of alkane SOA yield to *n*-dodecane SOA yield based on Lim and Ziemann (*7*), Lewandowski et al., SOA formation yields from the linear C_8 through C_{14} alkanes, *in preparation*, and Presto et al. (*1*). Ratio is taken at similar and/or atmospherically relevant loadings if possible. Values are available in Table S1.
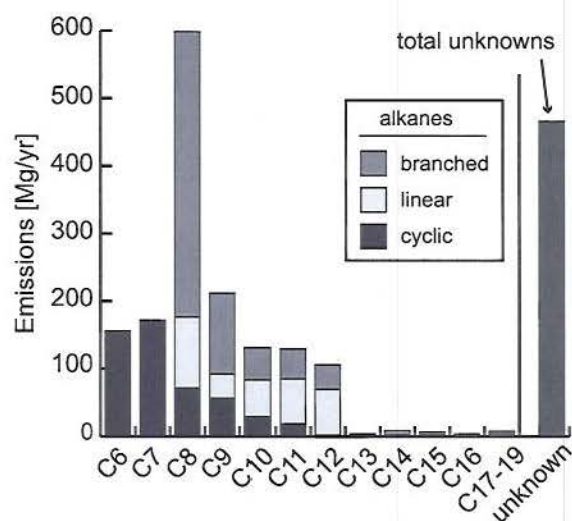
Figure 2: Domain-wide emissions of alkane SOA precursors by carbon chain length and structure and unknown/unidentified compounds.
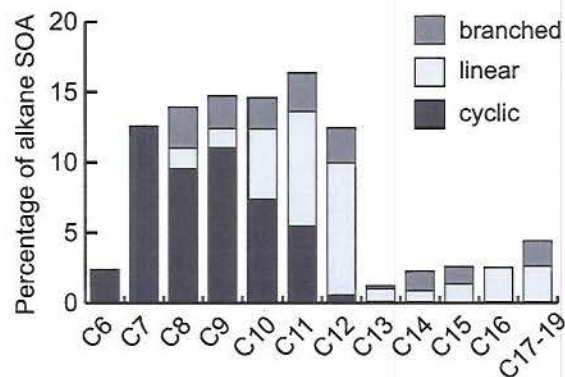

Figure 3: Estimated contribution of alkanes to SOA from alkanes by length and structure. Sum is 100%.
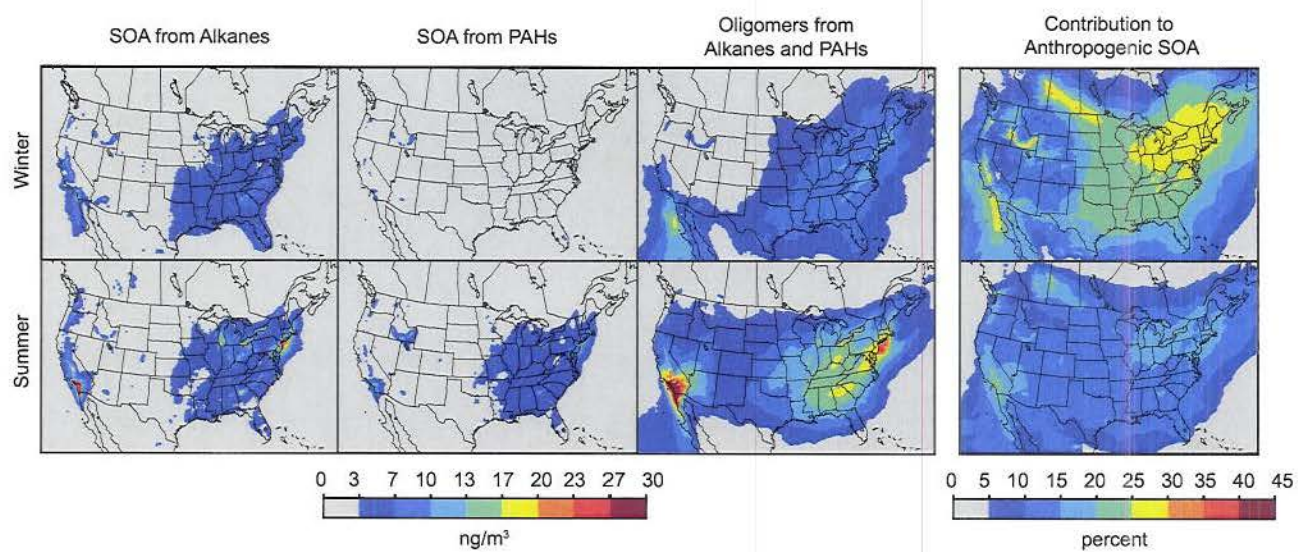
19

Figure 4: Predicted surface level SOA from alkanes, PAHs, and their oligomers as well as their contribution to surface level SOA from anthropogenic hydrocarbons. The top row is an average for January 11 through February 10 and the bottom row for July 1-31, 2006. See Figure S2 for a total of columns 1-3 and Figure S3 for the contribution to total SOA including biogenics.
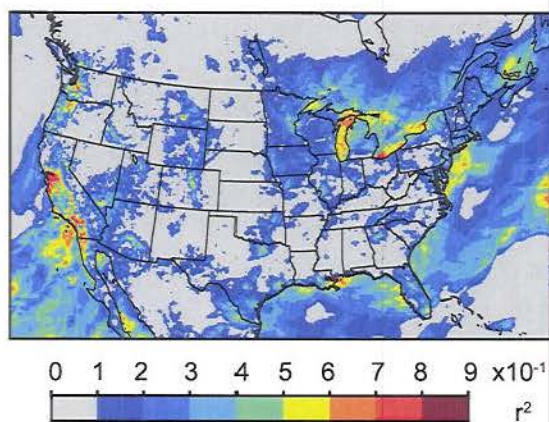
Figure 5: R-squared (r^2) between modeled SOA from alkanes (excluding oligomers) and odd oxygen (NO_2+O_3) based on hourly averages for July 2006.
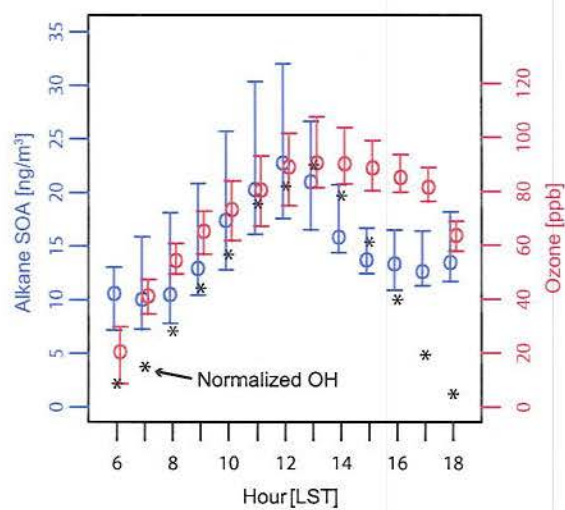

Figure 6: Alkane SOA, OH (normalized), and ozone concentrations binned by hour of day in Bakersfield, CA (-118.97° longitude, 35.35° latitude) for July 2006. Bars span the 25th and 75th percentiles and circles indicate the median. The median normalized OH by hour is plotted as stars for reference.